

Structural Performance of A 3D Reinforced Concrete Building Obtained By both Nonlinear Static and Dynamic Analysis

Anastasia K. Eleftheriadou

Postdoctoral Researcher, Xanthi, Greece

Corresponding Author: Anastasia K. Eleftheriadou

Abstract: *The paper presents thoroughly the process for the analytical estimation of reinforced concrete structures structural vulnerability. In order to achieve this purpose, both nonlinear static and dynamic analysis have been implemented on a 3D standard reinforced concrete moment resisting building and the seismic response is obtained analytically by both methods. The selected building for illustration was designed according to older seismic codes and regulations (Hellenic Code of 1959) and without conforming to modern seismic detailing requirements. The 3D model was subjected to conventional Static Pushover Analysis and bidirectional Incremental Dynamic Analysis (IDA) with the use of SAP 2000 software program. IDA involves nonlinear dynamic analyses of the structural model under a suite of ground motion records, each scaled to several intensity levels designed to represent the structure's behaviour ranging from elasticity to final global instability. The structural performance of the RC building under static and dynamic seismic loads was demonstrated in pushover, capacity, fragility and IDA curves which were obtained from the previous analyses. In addition, results of the two methods are compared and the assessed performances are discussed.*

Keywords: *Seismic response; Structural performance; Pushover analysis; Dynamic analysis; Vulnerability*

Abbreviations: *RC: Reinforced Concrete; IDA: Incremental Dynamic Analysis*

Date of Submission: 01-08-2018

Date of acceptance: 16-08-2018

I. Introduction

The destructive results of a strong earthquake in urban centres with densely concentrated population and buildings constitute valuable data for the efficient seismic risk assessment in individual level regarding the structural losses of each existing building type, and in general level regarding the total losses of the referring earthquake. The efficient earthquake resistance policy of urban planning poses as a priority the seismic strengthening (rehabilitation) of vulnerable structures and equivalently demands the reliable seismic assessment.

Earthquake loss estimation is a recently developing field wherein vulnerability curves can be regarded as a basic tool in estimating the expected damage of a future earthquake. In the present work, a methodology for assessing the seismic behavior of a structure designed according to older seismic codes and regulations [Greek Royal Decree of 1959, which served as the Seismic Code for this country up until 1985] is developed, its results consisting among other of fragility curves. In this way a complete risk assessment tool with a high degree of confidence can be applied to a wide range of reinforced concrete buildings representative of the pre-1980s design framework.

Structural performance was estimated under seismic loads by using both nonlinear Static Pushover Analysis and Incremental Dynamic Analysis. The method of Static Pushover Analysis based on Capacity Spectrum allows, using a suitable scaling of the static load or a target displacement that the structure must reach, the step-by-step observation of structural response, from elasticity to yielding and final collapse [FEMA 273 & 274, 1997, ATC-40, 1999]. The method's advantage is in the uniform investigation of structural response throughout the ranges of performance without "loss" of any of the characteristic points. On the other hand, Incremental Dynamic Analysis subjects the structural model to a suite of ground motion records, each scaled to several intensity levels especially selected to represent seismic performance of the structure from elasticity to final global instability [Vamvatsikos & Cornell, 2002]. The benefit of its application is mostly centred on the better understanding of structure's behaviour as the intensity increases whereas the consideration of different intensity levels is a basic tool for vulnerability assessment. Both types of analyses, i.e., static pushover and incremental dynamic analysis, were performed so as to examine the impact of seismic loads in the selected building. Results of the two methods are correlated and are used to construct vulnerability curves for buildings representative of typical South European substandard reinforced concrete construction in the 1970's.

1. Structural Model

1.1 Description of the structure

A 4-storey three-dimensional typical moment resisting reinforced concrete frame structure was used as a case study (Figure 1) in order to conduct a comparative investigation of performance of both the nonlinear static and dynamic method. The building was designed according to older codes and regulations [Greek Concrete and Seismic Codes of 1954 and of 1959 respectively) and is non-conforming to modern seismic detailing requirements and philosophy, thus becoming a representative sample of the pre-1980s design framework. It had a rectangular plan with 35.15m x 21.40m, five bays in the longitudinal direction and three bays in the transverse direction (Figure 2), and 11.4m of maximum height (2.85m per floor). This idealized frame model resembles in essentials the structural system of an actual building that underwent severe, non-recoverable damage during the 1999 Athens earthquake.

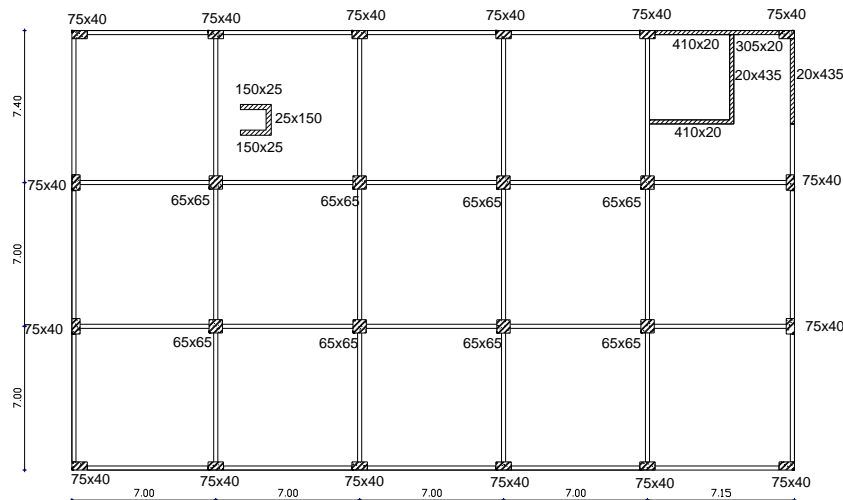


Figure 1: Plan of the building's frames

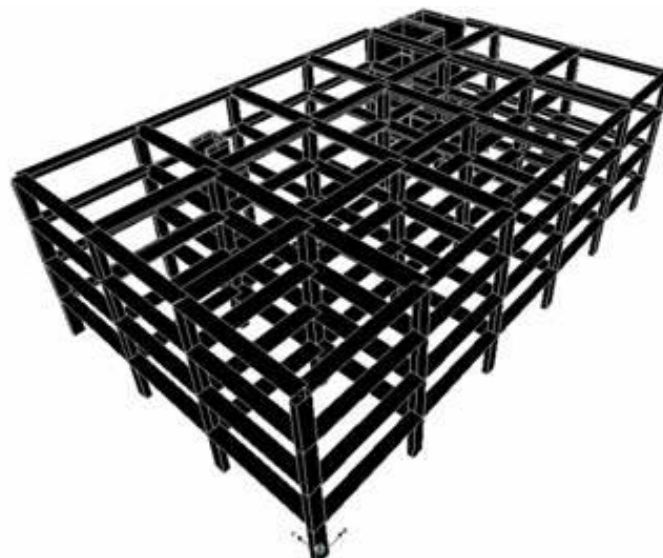


Figure 2: 3D outline of the building's frames

From experience and field data material mechanical properties are taken as follows: $f_c = 20\text{N/mm}^2$ uniaxial strength of concrete in compression with $\epsilon_{clim} = 0.0035$, using a stress-strain relationship for unconfined concrete as per the Model Code 90 [CEB-FIB, Model Code 90, 1990].

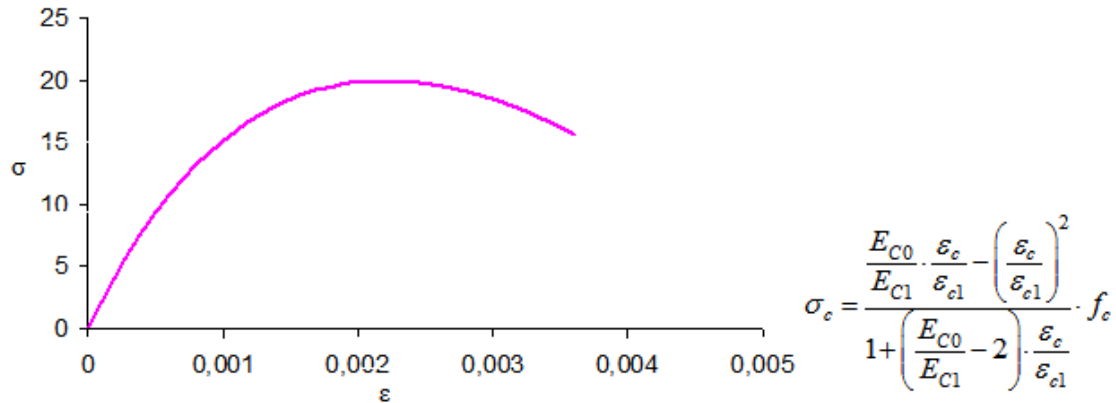


Figure 3: Stress-strain relationship for unconfined concrete.

Yield stress for the longitudinal and transverse reinforcement was taken as: $f_y=400 \text{ N/mm}^2$ and $f_y=220 \text{ N/mm}^2$, respectively. Flexural section analysis for all frame members was conducted using the Park-Sampson model for steel.

$$\sigma_s = f_y \cdot \left[\frac{m \cdot (\varepsilon_s - \varepsilon_{sh}) + 2}{60 \cdot (\varepsilon_s - \varepsilon_{sh}) + 2} + \frac{(\varepsilon_s - \varepsilon_{sh}) \cdot (60 - m)}{2 \cdot (30 \cdot r + 1)^2} \right]$$

$$m = \left[\frac{\frac{f_u}{f_y} \cdot (30 \cdot r + 1)^2 - 60 \cdot r - 1}{15 \cdot r^2} \right]$$

$$r = \varepsilon_{su} - \varepsilon_{sh}$$

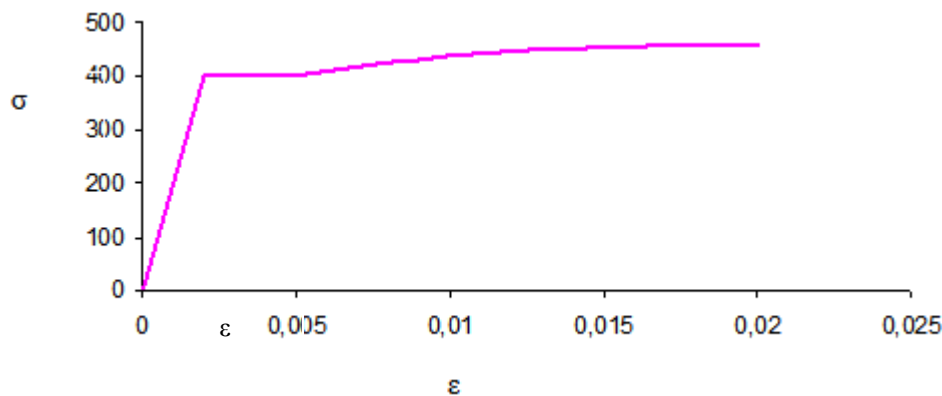


Figure 4: Stress-strain relationship for steel.

The structural system consisted of sixteen perimetric columns with cross section of 75cmx40cm (4Φ16+4Φ16), eight central columns with cross section of 65cmx60cm (4Φ20+4Φ20), two eccentric concrete walls (2Ø14+2Ø14, 2#Ø8/25) and slabs with 15cm of height (4Φ10/m) which were supported by beams with cross sections of 20cmx60cm (2Φ10up+2Φ14down). All structural elements are assumed to have closed stirrups of Φ6/30.

Effective structural stiffness was calculated assuming cracked sections with the concession that the estimated value remains constant over the entire length of the member according with the recommended values of the current Greek seismic code [Greek Seismic Code, 2000]: $EI_{ef} = 0.40EI_g$ for beams, $EI_{ef} = 0.60EI_g$ for perimetric columns and shear walls and $EI_{ef} = 0.80EI_g$ for the central columns, where I_g is the gross moment of inertia. The reinforced concrete slabs are assumed to ensure diaphragm action, as they did not have significant openings (except for the area of stairwell and elevator).

A uniformly distributed dead load of 1.5KN/m^3 is assumed superimposed on the self-weight of the structure whereas perimetric beams supported masonry walls with an estimated weight of 3.60KN/m^2 . In addition, live loads are represented by a uniformly distributed load of 2.0KN/m^3 . Distributed slab loads are assigned to beams according using partial moment redistribution [Greek Seismic Code, 2000].

1.2 Modal Analysis

The mass of structure was considered as distributed to the individual structural elements. In order to evaluate the total structure’s mass, gravity loads were superimposed to 30% of the nominal live load $M=P/g=(G+0.3Q)/g \text{ KN}\cdot\text{sec}^2/\text{m}$ [Greek Seismic Code, 2000]. After performing a modal analysis with a nonlinear structural analysis program [SAP2000, 2000], the fundamental period in direction xx was evaluated as $T_x=0.245 \text{ sec}$, associated with the prevailing mode of vibration of the structure in that direction (2nd global mode). The fundamental translational mode of vibration occurred in the yy-direction, with an associated period of $T_y=0.488 \text{ sec}$. The relevant data are outlined in Table 1.

Table 1: Modal Participation Mass Ratio of the first five modes

Mode	Period (sec)	Modal Participating Mass Ratio (%)	
		Ux	Uy
1	0.488	14.175	46.354
2	0.245	66.914	24.178
3	0.166	10.038	20.738
4	0.093	1.207	3.556
5	0.062	0.176	1.009

Assuming a soil type C, the spectral acceleration values corresponding to the fundamental structural periods in the two orthogonal directions of lateral translation were evaluated from the current code design spectra ($T_1=0.2$ and $T_2=0.8\text{sec}$). Thus, $\Phi_d(T_x)=\Phi_d(T_y)=0.6g$ in directions xx and yy. Finally, the base shear was estimated as $V_{ox}=V_{oy}=M*\Phi_d(T)=M*0.6g$.

Note that owing to the symmetric placement of the columns, the center of mass is considered to coincide with the geometric center of the plan. At that point, the base shear was triangularly distributed in each floor according to the equation $F_i=V_o*(m_i z_i / \sum m_i z_i)$ [Greek Seismic Code, 2000].

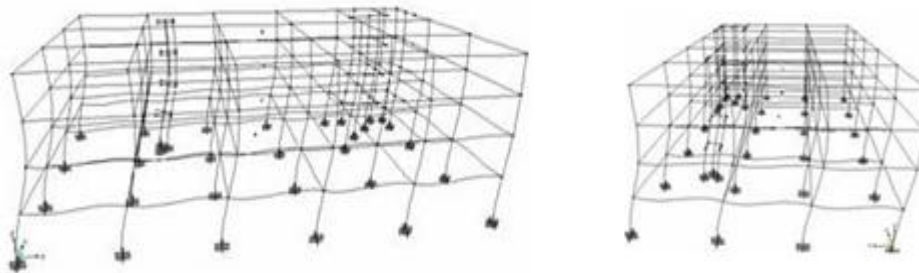


Figure 5: The first two modes.

1.3 Section Analysis

The structure was analyzed for four static combinations of loads: seismic loads V_x and V_y and seismic loads superimposed with gravity loads $G+0.3Q$. The structural elements with the same sections and similar internal forces were organized in groups. Several section analyses for all element groups, considering the heaviest internal forces, were then performed with the RESPONSE-2000 software analysis program [RESPONSE2000, 2001] and also using standard flexural section analysis calculations, as well. In this way the axial load – moment interaction and the moment-curvature diagrams for each cross section of the structural elements were obtained. The moment-rotation diagrams were derived using basic Mechanics with the approximate equation of Park & Priestley [Paulay and Priestley, 1992] for the plastic hinge length. Section analysis results were obtained for every section. An example is presented for a column 75/40 in Table 1.

For $\varphi \leq \varphi_y$: $\theta = 1/3 * \varphi * L_o$ (1)

For $\varphi > \varphi_y$: $\theta = \theta_y + \theta_p$ (2)

$$\theta_p = (\varphi_u - \varphi_y) * L_p \tag{3}$$

$$L_p = 0.08 * L_o + 0.0022 f_{ydb} \tag{4}$$

Where φ_y, φ_u : yield and ultimate curvature, respectively
 θ_y, θ_p : yield and plastic rotation angle, respectively
 L_o, L_p : shear span and plastic hinge length, respectively
 f_{ydb} : steel yield stress

Table 2. Results from the section analysis Αποτελέσματα από την ανάλυση των διατομών.

C 75/40	My	φ_y	Mu	φ_u	θ_y	θ_u	$V_y = My/l_s$	$V_u = Mu/l_s$
	KNM	1/mm	KNM	1/mm	rad	rad	KN	KN
1 st floor	206.144	7.85E-06	223.138	1.03E-04	3.73E-03	0.017	144.66	156.59
2 nd floor	178.54	7.13E-06	194.5	2.01E-04	3.39E-03	0.031	125.29	136.49
3 rd floor	149.8	7.13E-06	164.86	2.67E-04	3.39E-03	0.040	105.12	115.69
4 th floor	135.29	6.48E-06	149.15	2.93E-04	3.08E-03	0.044	94.94	104.67

In addition, based on the geometrical characteristics of the sections and the shear reinforcement, the real shear strength V_{rd} was evaluated for every structural element, from which the $M_{rd} = V_{rd} * l_s$ was then estimated. Analyzing the results occurred that shear failure was the predominant type of failure (Syntzirma & Pantazopoulou, 2003).

2. Non-Linear Static Pushover Analysis

2.1 Application of Static Pushover Analysis

In order to perform the Static Pushover Analysis using SAP2000 frame hinge properties should in advance be defined using the previous results of moment-rotation diagrams of structural elements [SAP2000, 2000]. Moreover, inelastic action should be restricted, in terms of plastic rotation angle, for the selected performance levels (immediate occupancy, life safety and collapse prevention) for the applied actions. Tables 6.7, 6.8 and 6.18 of FEMA 356 determine the numerical values of the performance levels for concrete beams, columns and shear walls, respectively [FEMA 356, 2000]. Using the component force versus deformation curves proposed by FEMA 356 a ductile behaviour for concrete beams, columns and short length shear walls was selected, where there is an elastic range followed by a plastic range that included strain hardening or strain-softening range and a strength-degraded range with no ability to support gravity loads beyond that. Long length shear walls were described using a bilinear curve that represents brittle non-ductile behaviour, with a linearly elastic range followed by loss of strength and loss of ability to support gravity loads.

After assigning hinge properties to the structural elements, the seismic loads which were concentrated in the centre of mass were applied incrementally until the structure reached a monitored displacement. In the program, a static analysis with gravity loads precedes the pushover analysis. P-delta effects were considered, whereas the analysis was performed separately in the two orthogonal axes.

2.2 Pushover Analysis Results

The results of Pushover analysis include information on the sequence of frame hinge formation. Thus, it is possible to observe those elements that are excessively strained. The capacity curve was obtained from the structural analysis with the real strengths and rotations in the modelling of plastic hinges. The capacity curve is defined by the yield displacement of the control point and by the ultimate displacement of the control point. From the structural response it is concluded that there is a shear failure due to the vertical structural elements

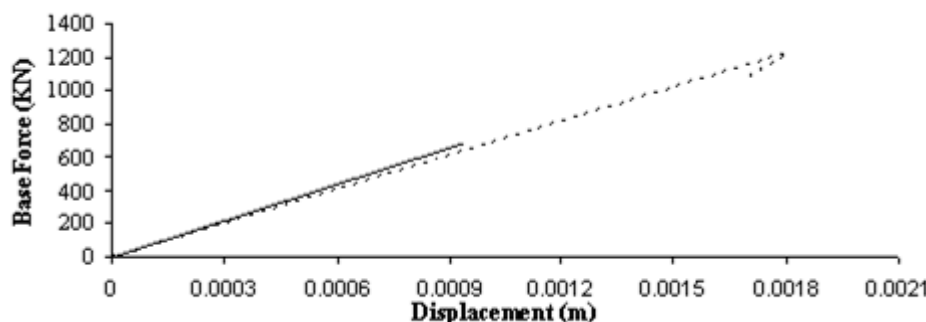


Figure 6: Pushover X and Y shear failure.

Ignoring the shear failure of the columns and considering that plastic hinges have a bending type failure the pushover capacity curves are developed for the two directions XX and YY. as shown in Figure 7, for the longitudinal and transverse directions, respectively. It was derived from a plot of static-equivalent base shear

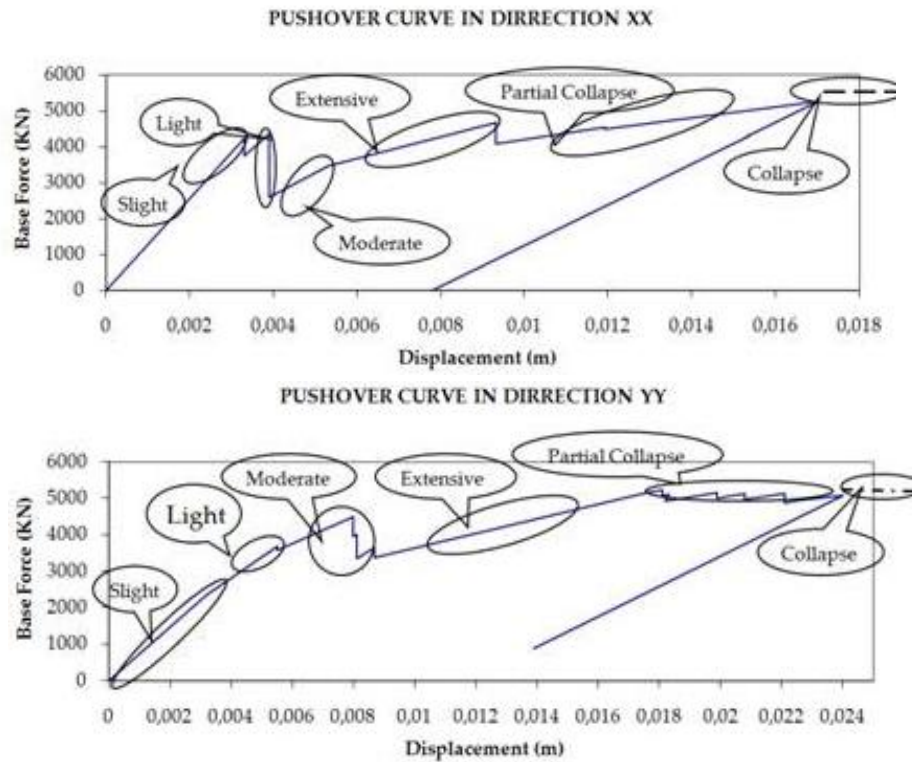


Figure 7: Damage-State Medians of “Saw-Tooth” Pushover Curve

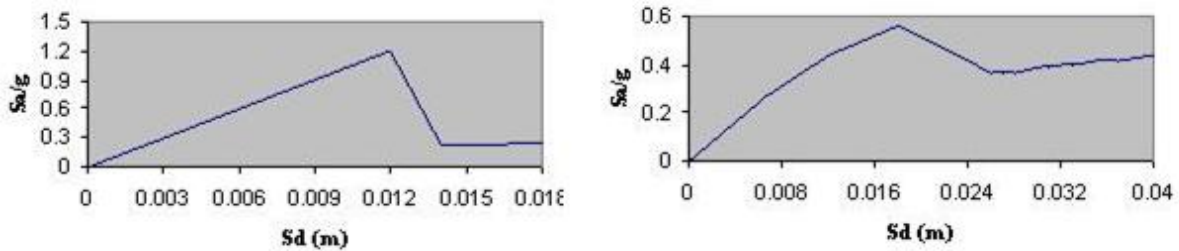
versus building displacement at the roof. The control node was located at the centre of mass of the highest floor (4th floor). Each capacity curve is defined by the yield displacement of the control point and by the ultimate displacement of the control point.

Examining the obtained pushover curves of the present building it was concluded that the structure sustained a load reduction in a number of components at different levels of base-shear. The sequential shear failure of components creates a “saw-tooth” effect (HAZUS^R99, 1999). Damage states could be also determined on the Pushover Curve according to the shape of the curve and the formation of plastic hinges. Thus, the median of slight damage is defined at the moment that the capacity of the first structural component on its load deformation curve drops. The median of moderate damage is defined when the capacity drops for additional components. Accordingly, the median of extensive and partially collapse damage refers to the stage where a substantial number of components have lost their capacity and the structure is in near collapse state, marginally sustaining the applied lateral forces. Collapse is assumed to occur when the building has lost its strength. Typically, a building is assumed capable of deforming beyond its ultimate point without loss of stability, but with no additional resistance to earthquake forces.

In order to facilitate a direct comparison with the spectral demand, the Pushover Curve is converted to Capacity curve [Pantazopoulou, 2003] using equations (5) and (6):

$$S\alpha = \frac{V / W}{\alpha_1} \tag{5}$$

$$Sd = \frac{\Delta_{top}}{PF_1 * \Phi_{1,top}} \tag{6}$$



(a) (b)
Figure 8: Capacity Spectrum in directions xx (a) and yy (b)

Where: S_a and S_d are spectral acceleration and displacement,
 W is the modal weight,
 $\Phi_{1,top}$ is the amplitude of mode 1 at roof level,
 α_1 is the modal mass coefficient for the first natural mode and
 PF_1 is the modal participation factor for the first natural mode.

SAP2000 has the ability to convert directly Pushover Curve to Capacity Curve. The Capacity Spectrum, of the examined building, for both directions reaches an ultimate point and then drops in order to continue with a “flat” line. Figure 9 shows the development of max inter-storey drift ratio developed in 2nd floor according to the sequence of the Pushover steps.

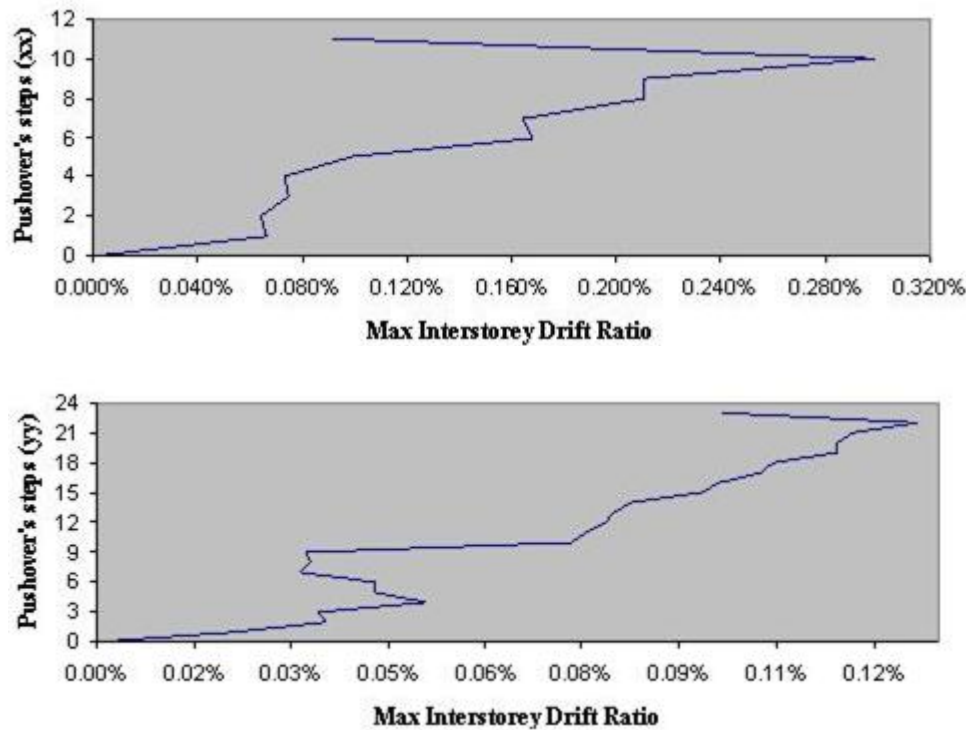


Figure 9: Development of max inter-storey drift ratio corresponding to the steps of the Pushover Analysis.

2.3 Fragility curves

From the predefined damage levels the fragility curves for the building model under examination were derived. These are lognormal cumulative Probability functions that describe the probability of reaching or exceeding a certain damage level. For the class of structures under investigation, six performance levels were considered: slight, light, moderate, extensive, partial collapse and collapse. Each fragility curve was defined by a median value of the demand parameter (e.g. spectral displacement) corresponding to the threshold of that damage state (DS) and by the variability β_{ds} associated with the same threshold of the damage state.

$$P[ds / Sd] = \Phi \left[\frac{1}{\beta_{ds}} \ln \left(\frac{Sd}{\overline{Sd}_{ds}} \right) \right] \tag{7}$$

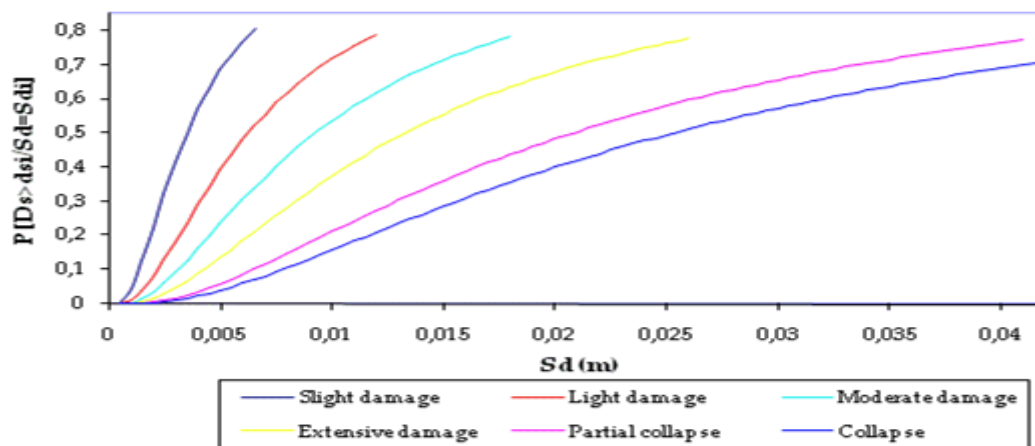
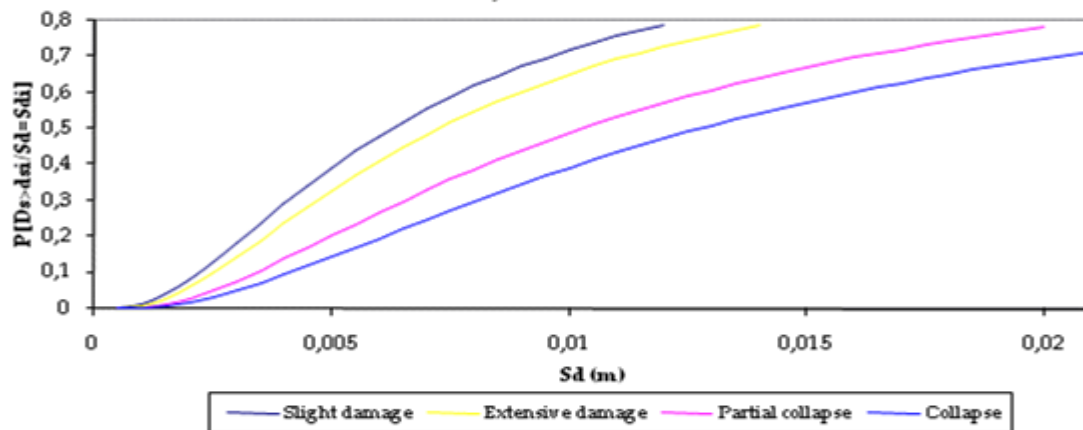
Where: β_{ds} is the standard deviation of the natural logarithm of spectral displacement for damage state ds ,
 \overline{Sd}_{ds} is the median value of spectral displacement at which the building reaches the threshold of damage state ds
 Φ is the standard normal cumulative distribution function

Figure 10 shows the damage probability of each damage state corresponding to the value obtained from the capacity curve. The relevant data for the median value and the standard deviation are given in Table 2. In direction xx, there is a progressive development of damage, therefore the first performance levels are omitted. In general, damage in both directions is developed for small spectral demand. Nevertheless, in transverse direction where there are fewer shear walls with the strong axis oriented in that direction, structural response develops larger values of deformation.

Table 3: Numerical values of β_{ds} and \overline{Sd}_{ds} in each damage state

	β_{ds}		\overline{Sd}_{ds}	
	xx	yy	xx	yy
Slight damage	0.812989	0.736747	0.00625	0.00351
Light damage	-	0.812989	-	0.00625
Moderate damage	-	0.853235	-	0.00925
Extensive damage	0.829253	0.883139	0.00725	0.01325
Partial damage	0.862406	0.912733	0.01025	0.02075
Collapse	0.880022	0.923400	0.01275	0.02525

(a)



(b)

Figure 10: Fragility Curves in directions xx (a) and yy (b)

III. Incremental Dynamic Analysis

3.1 Application of IDA

Incremental Dynamic Analysis (IDA) subjects a structural model to one or more ground motion records, each scaled to multiple levels of intensity, thereby producing one or more curves of response. Using a series of nonlinear dynamic analyses IDA attempts to establish thoroughly the building's performance under seismic loads observing structural response over the entire range from elasticity to global instability as the ground motion increases (Vamvatsikos & Cornell, 2002).

Two ground motion records were selected from the Athens 1999 earthquake as described in Table 2. Each of these has been scaled up and down so as to cover the entire range of structural response from elasticity, to yielding and finally to global dynamic instability. Thus, about 50 bidirectional nonlinear dynamic analyses (about twelve runs per record in each direction) were performed for the 3D standard reinforced concrete moment resisting building. During the analysis, scaling of the record was becoming more "dense" near the characteristic points (e.g. yield point).

Table 4: Recorded accelerograms used in the application.

Name	Date	Station name	PGA (m/sec ²)
Athens	7/9/1999	Sepolia Garage	2.7604
Athens	7/9/1999	Syntagma 1st	1.17

3.2 IDA's results

Once the analysis routine was completed a post-processing procedure was followed. From each run, a couple of values of structural demand versus the ground motion intensity level were selected. For the specific occasion, the maximum base shear force, in the direction that the record was applied, and the equivalent roof displacement were used as point of reference for the sake of comparison with the results of static pushover analysis. Thus an IDA curve was designed.

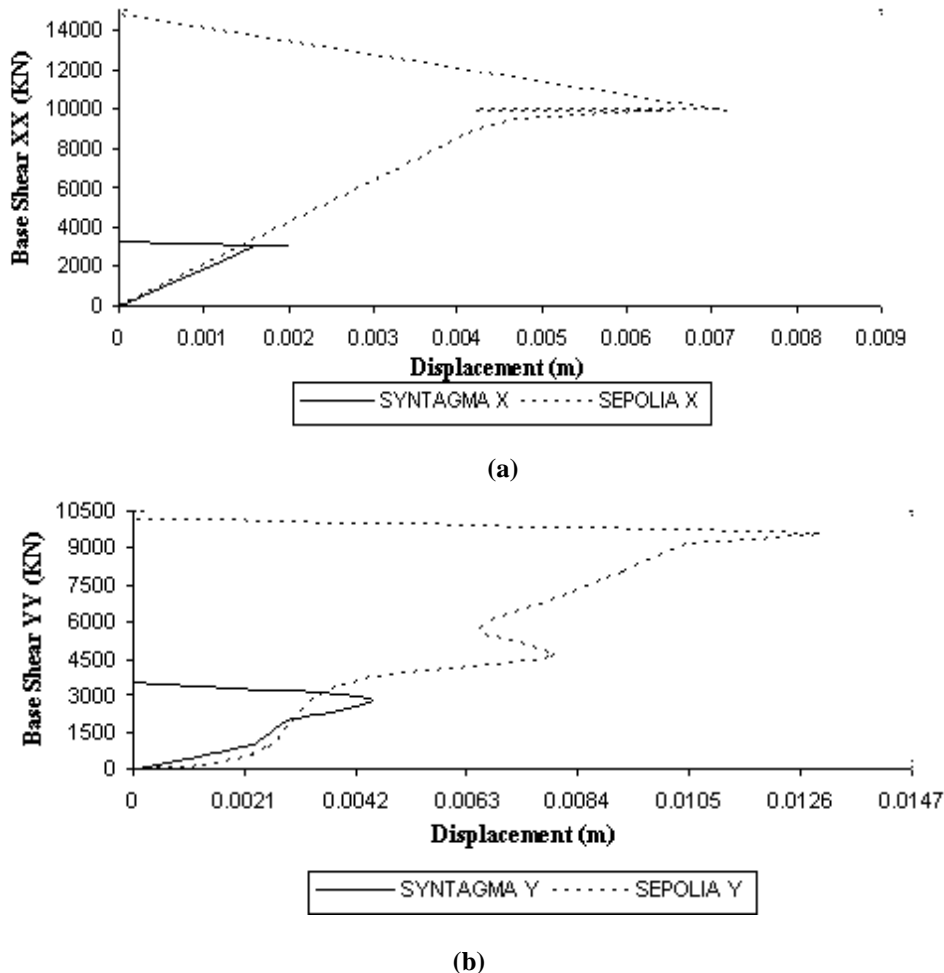


Figure 11: IDA Curves in directions xx (a) and yy (b)

In the longitudinal direction the IDA curve starts as a straight line in the elastic range and shows a ductile behaviour for a small “flat” region, when a reversal of the IDA curve is observed underscoring the influence of higher mode effects due to nonlinearity in the response. Similarly, in the transverse direction also an elastic region is observed, but after the yield point the IDA capacity curve weaves around the initial elastic slope, with the local slope of stiffness increasing and decreasing.

Each graph illustrates the demand imposed upon the structure by each ground motion at different intensities. All curves have an elastic linear region with similar elastic stiffness for the records applied in the same direction as it may be seen from the tangent slope of the base shear–control node displacement diagram. Observing the extreme end of the curves, it is observed that they terminate for different levels of base shear. There is also a difference in behavior resulting from the records that were applied. Thus, although structural response is similar in “quality” for the two records, they differ in “quantity”, namely the numerical values of the demand and the response.

3.3 Correlation between SPO and IDA results

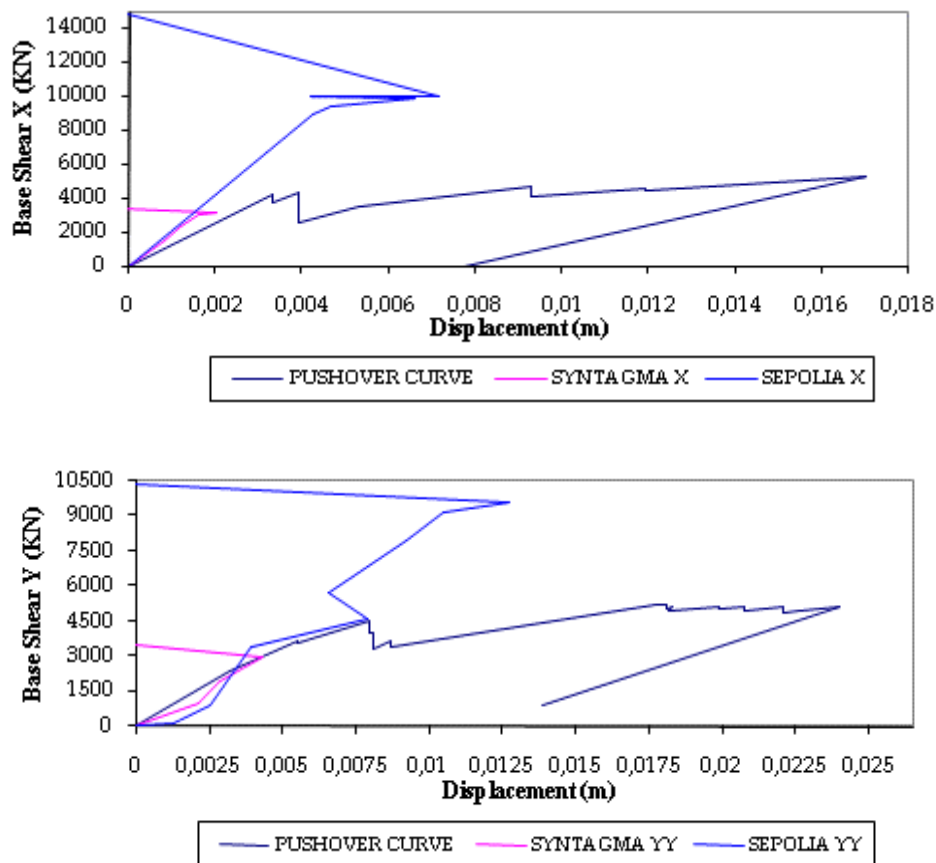


Figure12: Correlation between Static Pushover and IDA Curves

As both static and dynamic analyses refer to the same structure it was expected that results would be correlated or that at least the curves would possess some affinity with each other. The diagram of base shear versus roof displacement was used as a basis of comparison by plotting the results of the two analyses types on the same graph (Figure 8). Clearly, analysis results are similar while the demand is low enough for the structure to remain in the elastic range. The first saw-tooth strength drop in the pushover curve corresponds to the deviation of the IDA curve from the mean elastic slope, marked by weaving and snap back. Despite the qualitative resemblance, especially with Sepolia’s station accelerogram, there is almost no quantitative correlation, as the pushover curve sustained bigger deformation for lower seismic demand.

IV. Conclusions

A step-by-step static pushover and an incremental dynamic analysis have been performed using the SAP2000 software for a 3D standard reinforced concrete moment resisting building designed according to older seismic codes and regulations. Pushover, capacity, fragility and IDA curves were obtained from the

previous analyses in the effort to compare structural performance results obtained from different types of analysis under seismic loads. The relationship between the results of the alternative procedures is discussed; great differences are identified in the load-displacement response curves obtained from static pushover and the IDA upon the onset of first yielding. Clearly the number of records is not sufficient in order to provide stable estimates of the statistics of the response. The application of more accelerograms is proposed in this regard. In addition, values at failure are rather low consistent with the low deformation capacity of the structure owing to its poor detailing. It is also possible that using a more detailing modelling procedure where all other mechanisms of likely localised failure would be accurately reflected, could lead to even greater dispersion of the resulting capacity curve.

References

- [1]. ATC-40: Applied Technology Council, (1996), Seismic Evaluation and Retrofit of Concrete Buildings Volume 1, California Seismic Safety Commission, Volume I, Report SSC 96-01, Redwood City, California.
- [2]. Bonett, R., Barbat, Al. and Pujades, L. (2004), Seismic Fragility Curves for Traditional Unreinforced masonry buildings of Barcelona Spain, *Journal of Structural Engineering*, 1, n° 4, 3-11.
- [3]. CEB-FIP, Model Code 1990 (1990).
- [4]. GREEK CONCRETE CODE (1954), Athens, Greece.
- [5]. GREEK SEISMIC CODE (Greek Royal Degree of 1959) (1959), Athens, Greece.
- [6]. GREEK SEISMIC CODE (2000), Earthquake Protection and Planning Organization, Athens, Greece.
- [7]. FEMA 273 (1997), NEHRP Commentary on the Guidelines for the Seismic Rehabilitation of Buildings, FEMA, Washington.
- [8]. FEMA 274 (1997), NEHRP Commentary on the Guidelines for the Seismic Rehabilitation of Buildings, FEMA, Washington.
- [9]. FEMA 356 (2000), Prestandard and Commentary for the Seismic Rehabilitation of Buildings, FEMA, bWashington.
- [10]. HAZUS⁹⁹ (1999), Earthquake Loss Estimation Methodology Advanced Engineering Building Module, Technical and User's Manual, FEMA, Washington.
- [11]. Karabinis, A.J. (2005), Reinforced Concrete Structures, Demokritus University of Thrace, Xanthi,, Greece.
- [12]. Karayannis, C.G. (2005), Seismic Design of Reinforced Concrete Structures, Demokritus University of Thrace, Xanthi,, Greece.
- [13]. Moreno, R., Barbat, Al. and Pujades, L. (2004), Seismic Fragility Curves for Framed Buildings with Flat Beams, *Journal of Structural Engineering*, 1, n° 4, 36-43.
- [14]. RESPONSE-2000 Sectional Analysis Software Program, Toronto, Canada.
- [15]. RESPONSE-2000 Version 1.1(2001), User Manual, Toronto, Canada.
- [16]. Pantazopoulou, S. J. (2003), Deformation Capacity of Old-Components, Chapter 4, State of the Art Report Seismic Assessment and Retrofit of Reinforced Concrete Buildings, WG1, FIB Seismic Commission (C7-WG1), fib Bulletin #24.
- [17]. Syntzirma, D. and Pantazopoulou, S. J. (2003), Assessment of Deformability of Old-Type R.C. Members Using Capacity-Based Prioritizing of Failure Modes, CD-ROM Proceedings of the fib Symposium Concrete in Seismic Regions, Athens Greece.
- [18]. Paulay, T. and Priestley, M.J.N. (1992), Seismic Design of Reinforced Concrete and Masonry Buildings, John Wiley & Sons, New York.
- [19]. Penelis, G., Kappos, A. (2001), Seismic Resisting Concrete Structures, Publications Ziti, Thessaloniki.
- [20]. Pinto, P., Franchin, P., Lupoi, Al. and Lupoi, G. (2004), Seismic Fragility Analysis of Structural Systems, Proceedings of the 3rd International Workshop on Performance-Based Seismic Design, Bled, Slovenia.
- [21]. SAP2000 (2000), Integrated Finite Element and Design of Structures, Analysis Reference Manual, Computers and Structures, Inc. Berkeley, California, USA.
- [22]. SAP2000 Non linear Structural Analysis Program (2000), Static and Dynamic Finite Element Analysis of Structures Non Linear, Computers and Structures, Inc. Berkeley, California, USA.
- [23]. Singhal, A, Kiremidjian, A.S. (1996), Method for Probabilistic Evaluation of Seismic Structural Damage, *Journal of Structural Engineering*, 122, n° 12, 1459-1467.
- [24]. Vamvatsikos, D., Cornell, C.A. (2002), Incremental Dynamic Analysis, *Earthquake Engineering and Structural Dynamics*, 31, n° 3, 491-514.
- [25]. Vamvatsikos, D., Cornell, C.A. (2002), The Incremental Dynamic Analysis and its Application to Performance-Based earthquake engineering, Proceedings of the 12th European Conference on Earthquake Engineering, Paper 479.

Anastasia K. Eleftheriadou Structural Performance of A 3D Reinforced Concrete Building Obtained By both Nonlinear Static and Dynamic Analysis.” *IOSR Journal of Mechanical and Civil Engineering (IOSR-JMCE)* , vol. 15, no. 4, 2018, pp. 17-27